Supplementary information for:

The missing enzymatic link in syntrophic methane formation from fatty acids

Michael Agne, Sebastian Estelmann, Carola S. Seelmann, Johannes Kung, Dennis Wilkens, Hans-Georg Koch, Chris van der Does, Sonja Albers, Christoph von Ballmoos, Jörg Simon, and Matthias Boll*

*Corresponding author: Matthias Boll
Email: matthias.boll@biologie.uni-freiburg.de

This PDF file includes:

Supplementary Materials and Methods

Materials. The chemicals used were of analytic grade and were purchased from Fluka (Buchs, Switzerland), Merck (Darmstadt, Germany), Roth (Karlsruhe, Germany), Sigma-Aldrich (St. Louis, MO), AppliChem (Darmstadt, Germany), and Bio-Rad (Hercules, CA). 2,3,-Dimethyl-1,4-naphthoquinone (DMN) was synthesized as described (1), 2,3,6-trimethyl-1,4-naphthoquinone (TMN) according to the method reported in (2). CoA esters were synthesized from the respective free acids as described (3).

Cultivation of bacteria and cell fractionation. *S. aciditrophicus* strain SB (DSMZ 26646) cell mass was obtained as described before by anaerobic cultivation in the 200 L scale in a mineral salt medium with crotonate (30 mM) as sole carbon and energy source (4). Until further usage, cell material was stored in liquid nitrogen. For cell fractionation, cells were suspended in extraction buffer (0.5 g wet mass mL^{-1}) plus spatula tips of DNAse I, lysozyme, and dithioerythritol. Cell disruption was performed by a passage through a French pressure cell (American Instrument Company, Hartland, WI) at 1,100 Psi. Unopened cells were sedimented by a centrifugation at 2,000 *g* (30 min, 8 °C). Soluble cell extract and crude membranes were separated by a centrifugation at 200,000 *g* (1 h, 4 °C). Membranes were washed by homogenizing them in at least 2 mL extraction buffer per g cell wet weight followed by another centrifugation at 200,000 *g* (1 h, 4 °C). Washed membranes were homogenized in an aqueous solution suitable for further usage. All steps were performed anaerobically at 4 – 8 °C.

To prepare inner membranes for inside-out vesicles, the supernatant of extracts after 2,000 *g* centrifugation was layered on top of a sucrose density step gradient prepared in extraction buffer (bottom up: 4 mL 51%, 0.8 mL 45 %, 0.8 mL 36 %, up to 4 mL sample in 10 mL centrifugation tubes). After a centrifugation at 250,000 *g* (30 min, 4 °C) in a fixed angle rotor, a turbid brownish layer was collected between approximately 3.5 and 5.5 mL from bottom. The collected fractions were diluted 1:5 with extraction buffer and sedimented by centrifugation at 200,000 *g* (1 h, 4 °C). Pellets were homogenized in extraction buffer, frozen in liquid nitrogen and stored at –70 °C. The isolation of inner membranes was performed anaerobically at 4 - 8 °C with buffer R_{B2} (10 mM HEPES, 0.5 mM KCl, 100 mM NaCl, pH 7.5) as extraction buffer.

Enrichment of proteins. ETF was enriched under anoxic conditions from soluble cell extract with HEPES (10 mM, pH 7.8) containing 50 µM FAD as extraction buffer. Cell extract was applied to a DEAE Sepharose Fast Flow column (GE Healthcare, Chalfont St Giles, GB) equilibrated with buffer A (10 mM HEPES, 50 µM FAD, 10 % (v/v) glycerol, pH 7.8). Protein was eluted with 60 mM NaCl. To this fraction, saturated ammonium sulfate solution (pH 7.8) containing 1 mM EDTA was added drop-wise while stirring on ice, until 45 % saturation was reached. Precipitates were removed by centrifugation at 2,000 *g* (10 min, 8 °C). The filtrated supernatant was applied to a Phenyl Sepharose Fast Flow column (GE Healthcare) equilibrated with buffer B (buffer A plus 2 M ammonium sulfate). ETF was present in the second half of the flow through. Finally, unbound FAD was removed by passing the concentrate over a PD Mini-Trap G-25 desalting column (GE Healthcare).

EMO and mFDH were enriched under anoxic conditions from washed *S. aciditrophicus* membranes with buffer TB (20 mM Tris-HCl, 5 mM $MgCl_2$, pH 7.8) as extraction buffer. Solubilization buffer (buffer TB plus 3 % (w/v) n-dodecyl-β-D-maltoside (DDM)) was added dropwise until a detergent:protein ratio of 3:1 (w/w) was reached. The emulsion was stirred further for one hour at 8 °C. The supernatant obtained after centrifugation at 200,000 *g* (1 h, 4 °C) was applied to a DEAE Sepharose Fast Flow column (GE Healthcare) equilibrated with buffer TB plus 0.02 % (w/v) DDM. The fraction eluting between 220 and 350 mM was applied to a Superdex 200 gel filtration column (GE Healthcare) equilibrated with buffer TB plus 0.02 % (w/v) DDM and 250 mM NaCl. Here, mFDH eluted shortly ahead of EMO. Fractions showing a band at the expected heights during SDS-PAGE were pooled and stored at –70 °C. Enriched bands of mFDH and EMO were excised, tryptically digested, and analyzed by mass spectrometry (see below). The α-subunit (SYN_00602+3, α-subunit, erroneously annotated to two genes due to the selenocystein encoding UGA stop codon), and β-subunit SYN_00604 of mFDH were identified with 47 % and 15 % coverage, respectively, by MS analyses of tryptic peptides; EMO (SYN_02638) was identified with a sequence coverage of 54 %.

CHCoA DH of *S. aciditrophicus* was heterologously produced in *E. coli* with a C-terminal 6x His tag and purified as described before (4).

Protein analysis and quantification. To follow protein enrichments, protein preparations were routinely subjected to SDS-PAGE (12.5 % acryl amide gels) (5) and stained with Coomassie. Gel pictures were acquired with a ChemiDoc XRS+ and the Image Lab 3.0 software (Bio-Rad, Hercules, CA). To verify protein identities, the respective bands were excised and proteins were prepared for LC-MS analysis by tryptic in-gel digest accompanied by the reduction by dithiothreitol and alkylation of cysteine residues with iodoacetamide (see below). Protein concentrations were determined by the Bradford method (6) or with the Roti-Quant Universal kit (Carl Roth, Karlsruhe, Germany; for detergent containing samples) by comparison to a BSA standard curve.

For analysis of the subunit architecture, solubilized and enriched protein was subjected to blue native PAGE as described (7). Heme staining of EMO bands was as previously reported (8).

Quinone analysis. Quinones were extracted from 10 mL crude *S. aciditrophicus* membranes (1 g cell wet weight per mL H_2O) by the addition of 40 mL MetPet solution (methanol, petroleum benzene 50 - 70 °C boiling point, 1:1 (v/v)) and 5 mL acetone. After incubation at 37 °C for 30 min, while shaking at 140 rpm, phase separation was achieved by centrifugation at 600 *g* for 5 min. The top organic layer was collected, while the lower aqueous layer was extracted again with 40 mL MetPet solution as described above. Both organic layers were pooled and washed by the addition of 80 mL of a methanol/water mix (95:5 (v/v)), by shaking vigorously followed by discarding the lower phase. After evaporation of the solvent overnight, the remnants were resolved in 100 µL isopropanol. The identity of the quinones was determined by UPLC-PDA and UPLC-MS.

Heterologous MenK expression in *E. coli.* The *menK* gene of *S. aciditrophicus* (WP_011418586.1) was amplified by PCR (forward primer: AGTTAAGTATAAGAAGGAGATATACATATGATTTCAACCCTTGTCGGTTATA-TGGCCCG, reverse primer: TCACTTTTCGAACTGCGGATGGCTCCATGCACTCAA-TTCTTCCACAGGCAACCGCGTCTGC) using intact cells of *S. aciditrophicus* SB as template. The purified gene was ligated with a PCR-generated vector fragment of pACYCDuet-1 (Novagen; forward primer: ATGTATATCTCCTTCTTATACTTAAC, reverse primer: GTGCATGGAG-CCATCCGCAGTTCGAAAAGTGAAATAATCGAGTCTGGTAAAGAAACCGCTGCTGCG) using the NEBuilder HiFi DNA Assembly Master Mix (New England Biolabs, Ipswich, MA). Cell cultivation, quinone extraction and analysis with RP-HPLC was done as described before (9).

Measurement of pmf formation. The formation of a pH gradient at membrane vesicles was followed by fluorescence quenching of 9-amino-6-chloro-2-methoxyacridine (ACMA) with a FluoroMax-4 spectrofluorometer (Horiba, Kyoto, Japan; excitation wavelength 410 ± 2 nm, emission wavelength 475 ± 1 nm) using disposable cuvettes (semi-micro PS, Ratiolab, Dreieich, Germany) at 30 °C. 0.1 mg membrane vesicles were suspended in 1.5 mL buffer R_{B2} containing 2.5 mM $MgCl_2$ and 0.4 µM ACMA. The reaction was started by the addition of 0.5 mM ATP or pyrophosphate, respectively. Uncoupling of the membrane potential was induced by adding 33 mM NH_4Cl or 1 µM nigericin. Negative controls were additionally supplemented with 1 µM nigericin and valinomycin or 10 µM carbonyl cyanide *m*-chlorophenyl hydrazone (CCCP) before the reaction was started.

Spectroscopic methods. UV/visible spectroscopic data were acquired with a UV-1800 spectrophotometer (Shimadzu, Kyoto, Japan) using quartz cuvettes (diameter 1 cm) and analyzed using UVProbe software version 2.43 (Shimadzu).

LC-based analytic methods. Samples for LC analysis of reaction intermediates were routinely prepared by precipitating proteins by the addition of 2 volumes of methanol and centrifugation at 15,000 *g*. LC analysis coupled to UV/visible detection was performed with an Acquity H-class UPLC system (Waters, Milford, MA) and a photodiode array detector (PDA, Waters). LC-MS analysis was performed with an Acquity I-class UPLC system (Waters) coupled to a Synapt G2-Si Q-TOF mass spectrometer (Waters). PDA measurements were evaluated with Empower 3 (Waters), MS measurements were evaluated with MassLynx V4.1 (Waters), proteins were identified with PeptideLynx Global Server (Waters).

For LC-PDA analysis of CHCoA and CHeneCoA, 6 µL sample were applied to an Eurosphere II C_{18} reverse phase column (100 x 2 mm, Knauer, Berlin, Germany) maintained at 25 °C at a flow rate of 0.25 mL min^{-1} with 10 % acetonitrile in 10 mM potassium phosphate buffer (pH 6.8). After 1 min run time, the acetonitrile concentration increased linearly to 20 % within 0.5 min, then to 30 % within 2.6 min.

For LC-MS analysis of ETF cofactors, 8 µL sample were applied to a HSS T3 1.8 µm C_{18} reverse phase column (100 x 2.1 mm, Waters) maintained at 30 °C at a flow rate of 0.3 mL min^{-1} with 1 % acetonitrile/0.1 % formic acid (v/v) in water/0.1 % formic acid (v/v). After 2 min run time, the acetonitrile/0.1 % formic acid concentration increased linearly to 70 % within 1.5 min, then to 80 % within 2 min. The mass spectrometer with electron spray ionization was operated in the Resolution mode with positive polarity and a capillary voltage of 3 kV, a cone voltage of 40 V, 80 V source offset, 150 °C source temperature, 450 °C desolvation temperature, 1000 L h^{-1} desolvation gas flow (N_2), 100 L h^{-1} cone gas

flow (N_2) as well as 6 bar nebulizer pressure. Collision induced dissociation of precursor ions was performed using a trap collision energy of 20 V and argon gas after quadrupole-based selection of the respective m/z (LM resolution: 14.7).

For LC-MS analysis of quinones, a 2 µL sample was applied to an Eurosphere II C_{18} reverse phase column (100 x 2 mm, Knauer) maintained at 30 °C and 35 % isopropanol/65 % acetonitrile at a flow rate of 0.2 mL min^{-1} for 30 min. The mass spectrometer equipped with atmospheric pressure chemical ionization was operated in the resolution mode with positive polarity and a corona current of 15 µA, a cone voltage of 20 V, 60 V source offset, 380 °C probe temperature (most critical parameter), 600 °C desolvation temperature, 1000 L h^{-1} desolvation gas flow (N_2), 30 L h^{-1} cone gas flow (N_2) as well as 6 bar nebulizer pressure. Collision induced dissociation of precursor ions was performed using a trap collision energy ramp of 20 - 80 V and argon gas after quadrupole-based selection of the respective m/z (LM resolution: 14.7).

For the identification of peptides by LC-MS, 10 µL sample were applied to a Peptide CSH 1.7 µm C_{18} column (150 x 2.1 mm, Waters) at a flow rate of 0.04 mL min^{-1} with 1 % acetonitrile/0.1 % formic acid (v/v) in water/0.1 % formic acid (v/v). After 2 min run time, the acetonitrile/0.1 % formic acid concentration increased linearly to 40 % within 38 min, then to 85 % within 2 min. The mass spectrometer with electron spray ionization was operated in the $HDMS^E$ Resolution mode with positive polarity and a capillary voltage of 3 kV, a cone voltage of 25 V, 40 V source offset, 120 °C source temperature, 350 °C desolvation temperature, 800 L h^{-1} desolvation gas flow (N_2), 50 L h^{-1} cone gas flow (N_2) as well as 6 bar nebulizer pressure. Collision induced dissociation of precursor ions was performed using a transfer collision energy ramp of 20 - 45 V and argon gas. Peptides were identified by the PeptideLynx Global Server (Waters) and mapped against the translated genome of *S. aciditrophicus* SB (taxonomic identifier 56780) downloaded from UniProt.

Protein cofactor determination. All cofactor determinations were performed in biological triplicates, and are given as mean value ± standard deviations. Cofactors of ETF were extracted by an acidic protein precipitation in the absence of oxygen: 100 µg ETF were mixed with sulfuric acid (20 mM) and triethanolamine (10 mM, pH 7.7) in a total volume of 120 µL. The preparation was kept in dark for 25 min at 8 °C while shaking. After a centrifugation at 15,000 *g* (10 min, 4 °C), the supernatant was collected and kept in dark, while the pellet was suspended in 30 µl sulfuric acid (20 mM), followed by incubation and centrifugation as before. The pooled supernatants were analyzed with UPLC-MS or UPLC-PDA. FAD and AMP standards were analyzed accordingly.

Non-heme iron was determined colorimetrically (10). The determination of heme *b* was carried out spectroscopically under anoxic conditions: 408 µL EMO (1.8 µM) were mixed with 202 µL pyridine and 65.5 µL NaOH (1 M). UV/visible spectra were recorded in the fully reduced or oxidized state (titration with sodium dithionite or $K_3[Fe(CN)_6]$ solution). The concentration of heme *b* was calculated from the pyridine hemochrome spectrum using ε_{556}(reduced – oxidized) = 28.32 mM^{-1} cm^{-1} (11).

Redox potential determinations. The midpoint redox potentials of the heme *b* cofactors of EMO were determined by a stepwise reduction of an EMO/redox dye mixture with sodium dithionite while recording UV/visible spectra. The redox state of heme *b* was calculated by dividing the absorption at 427 nm by the absorption at 410 nm. The redox potential was determined by calculating the reduced-to-oxidized ratio of the redox dyes. Hereby, the amount of oxidized dye was derived from the absorption change at wavelengths at isosbestic points of heme *b* as follows: 420 nm (9,10-anthraquinone-2,6-disulfonate), 569 nm (indigotetrasulfonate, indigo carmine and methylene violet 3RAX) and 664 nm (methylene blue).

To determine the redox mid potential of CHeneCoA/CHCoA, a 1:1 mixture of CHeneCoA and CHCoA was added to a RP solution containing 4 µM CHCoA DH and an excess of redox dye pre-reduced by different amounts of sodium dithionite. The solution was incubated at 30 °C for up to 4 hours. At different time points the ratio of CheneCoA/ChCoA was determined by UPLC-PDA to obtain the equilibrium concentrations. The redox potential of each approach was calculated from the absorption at 492 nm (iodonitrotetrazolium chloride) or 612 nm (indigo carmine) of a 1:20 diluted RP solution.

Formation of liposomes. *E. coli* total lipids extract (Avanti Polar Lipids, Alabaster, AL) were purified by a precipitation step with acetone and a washing step with diethyl ether (12). Purified lipids were solved in chloroform and stored under a nitrogen atmosphere at –20 °C. For liposome formation, the solvent was removed thoroughly. The resulting lipid film was suspended in 2.5 mL buffer R_{B2} and subjected to six freeze/thaw cycles with liquid nitrogen versus 25 °C. Liposomes were stored at –70 °C.

Reconstitution of EMO in liposomes. Liposomes were diluted to 5 mg lipids mL^{-1} and made uniform in size by 11 passages through an extruder equipped with a Nucleopore polycarbonate filter with 0.1 µm pore diameter (Whatman, Little Chalfont, UK). Between 30 - 120 µg EMO were added to 250 µL liposome suspension in an N_2/H_2 (95:5) atmosphere followed by an incubation at 8 °C for 30 min. The detergent introduced with the EMO preparations was removed either by passage through a desalting column (PD MiniTrap Sephadex G-25, GE Healthcare) or by applying detergent-adsorbing beads (Bio-Beads SM-2 20-50 mesh, Bio-Rad, Hercules, CA). Beads were added in three portions to the reconstitution mixture (20, 50 and 60 mg). After each step the mixture was incubated for at least 30 min while it was mixed continuously by turning the whole reaction tube.

To monitor EMO reconstitution, proteoliposomes were layered on top of a sucrose density step gradient prepared in buffer R_{B2} (bottom up: 1 mL 65 %, 0.5 mL 26 %, 1 mL 13 % in 10 mL centrifugation tubes). After centrifugation at 200,000 *g* (45 min, 4 °C) in a fixed angle rotor, the gradient steps were collected separately and analyzed for protein content.

Analysis of electron transfer activities. All electron transfer processes were analyzed in an N_2/H_2 (95:5) atmosphere (with the exception of hydrogenase) at 30 °C in MOPS buffer (25 mM, pH 7.3) unless otherwise stated.

Electron transfer from formate to ETF or CHeneCoA was followed by the change of FAD absorption at 460 nm (ε_{460} [semi quinone state – reduced] = 1.4 mM^{-1} cm^{-1}) or by analysing CoA esters by UPLC-PDA, respectively. *S. aciditrophicus* washed membranes (0.5 mg protein mL^{-1}) were mixed with 1 mM sodium formate and 30 µM ETF as well as 5 µM CHCoA DH and 0.1 mM CHeneCoA in the latter case. For inhibition studies, 60 µM 2-Heptyl-4-hydroxyquinoline N-oxide (HQNO, stock solved in ethanol) were present in the assay mix.

CO_2-dependent NADH oxidation was followed by the decrease of NADH absorption at 340 nm (ε_{340} = 6.5 mM^{-1} cm^{-1}). Therefore, 5-20 µL *S. aciditrophicus* soluble cell extract was mixed with 0.225 mM NADH and 125 mM sodium bicarbonate in a total volume of 500 µL potassium phosphate buffer (250 mM, pH 6.5).

NAD^+ or DMN dependent hydrogenase and FDH activities were determined spectroscopically using stoppered glass cuvettes under a N_2 atmosphere. 10 - 20 µL of enriched enzyme, *S. aciditrophicus* soluble cell extract or washed membrane were diluted in 450 µL MOPS buffer (25 mM, pH 7.3) containing 2 mM NAD^+ or 90 µM DMN, respectively. The reaction was started by the addition of either 2 mM sodium formate or 200 µL H_2/CO_2 (80:20) by a syringe and followed at 340 or 272 nm (DMN, ε_{272} = 16 mM^{-1} cm^{-1}).

The NAD^+ dependent β-hydroxybutyryl CoA dehydrogenase activity of *S. aciditrophicus* soluble cell extract was tested aerobically at 37 °C. The reaction mixture contained 100 mM Tris-HCl (pH 8.0), 10 mM $MgCl_2$, 5 mM dithiothreitol, 0.5 mM NAD^+ and 0.5 mM β-hydroxybutyryl-CoA in a total volume of 500 µL. The reaction was started by the addition of 2.5 - 10 µL cell extract and followed at 365 nm (ε_{365} = 3.4 mM^{-1} cm^{-1}).

Electron transfer between ETF and CHCoA/CHeneCoA was followed by the change in FAD absorption at 460 nm (ε_{460} [semi quinone state – reduced] = 1.4 mM^{-1} cm^{-1}) with 15 µM ETF, 30 nM CHCoA DH and 0.1 mM CHCoA or CHeneCoA.

Heme *b* reduction was followed spectroscopically by adding 3 µM solubilized EMO or 0.7 µM EMO reconstituted in 2.5 mg mL^{-1} liposomes to buffer R_{B2} in a total volume of 130 µL. While recording spectra 6 µM ETF and 2 µM CHCoA DH, 0.1 mM CHCoA (pH 7.0 - 7.5) and 0.2 mM sodium dithionite were added sequentially.

For oxidation of reduced heme *b* by TMN, 2.5 µM EMO (with 3 [4Fe-4S] clusters and 2 heme *b*) was completely reduced by a slight excess of sodium dithionite redox equivalents (11 µM) in buffer R_{B2}. After each addition of TMN dissolved in DMSO (2 - 70 µM steps) spectra were recorded every 20 sec until the change of absorption at 413 nm was below 0.0004. The concentration of oxidized TMN was calculated by subtracting the concentration of excess dithionite from the total TMN concentration.

The electron transfer activity of EMO was determined by following the TMN dependent ETF reduction at 375 nm (ε_{375}[semi quinone state – reduced] = 0.88 mM^{-1} cm^{-1}). The reaction mix contained 30 µM ETF and 50 µM TMN previously reduced with 20 µM sodium dithionite in buffer R_{B2} and was started by the addition of 0.4 - 1.6 µM EMO.

Computational analyses. Protein sequence alignment was performed by BLASTp (13) using the sequence alignment option. Conserved domains were identified by the NCBI conserved domains web application (14). Transmembrane helices were predicted by the TMHMM server (15).

Protein structure homology models for the trans-membrane domain of EMO (residues 1- 270, template: NarI of *E. coli*) as well as the β and γ subunits of mFDH (separately for each subunit, templates: FdnH or FdnI of *E. coli*), were created by the servers Phyre2 (16), iTASSER (17), SwissModel (18) and raptorX (19) with standard parameters. Further evaluation and visualization were done with PyMOL (The PyMOL Molecular Graphics System, Version 2.3.2 Schrödinger, LLC): Structural alignments were performed by the Superposition/Alignment tool (5 cycles, cutoff 2.0, outlier rejection enabled). Surface charge was calculated by the APBS Electrostatics plugin (method: pdb2pqr, grid spacing: 0.5, range: +/- 5.0, Connolly surface).

A phylogenetic consensus tree was generated for EMO-like proteins. Sequences were selected by a BLASTp search with the amino acid sequence of EMO against the non-redundant protein sequences data base excluding models with a query coverage cut-off at 85 %. The first 9,300 results were subjected to the CD-HIT suite (20) to reduce the number of sequences to 600 while maintaining the evolutionary diversity. To include also more remotely related sequences, another BLASTp search was performed with the same parameters but the sequence with the highest E value of the first search as query. This step was repeated one more time. All sequences of this run, that were assigned with E-values between e^{-120} and e^{-60} during BLASTp analysis were subjected to the CD-HIT suite to reduce the number of sequences to 70. The selected sequences were pooled and further reduced by omitting those which were not assigned to a specific organism. To ensure that the whole distribution of EMO in the tree of life is depicted and to assess the scientific impact of the enzyme, its sequence was also subjected to a BLASTp search against selected organisms, which are syntrophic fatty acid degraders, pathogens, common model organisms, and prominent representatives of until then underrepresented organism classes. Sequences were selected, if their sequence coverage was above 85 % and their E-value was below e^{-60}. With all selected sequences a multiple alignment (ClustalW with Gap Opening Penalty: 10, Gap Extension Penalty = 0.1 for pairwise or 0.2 for multiple alignment, Negative Matrix = off, Delay Divergent Cutoff = 30 %) was performed using MEGA-X version 10.1.7 (21). This alignment was inspected manually while sequences with missing or disrupted trans-membrane helices, missing cysteine residues in conserved [FeS] cluster binding motifs or less than two conserved histidine residues in the trans-membrane domain were rejected. For rooting of the tree, HdrDE from *Methanosarcina acetivorans* was added as a fused protein with HdrE at the N-terminus. A phylogenetic consensus tree was constructed based on this alignment using the IQ-TREE web server

version 1.6.12 (22) (automated Substitution Model selection; Bootstrap analysis: Ultrafast with 1000 bootstrap alignments, maximum number of 1000 interations, minimum correlation coefficient of 0.99, SH-aLRT branch test with 1000 replicates; Perturbation strength: 0.5; IQ-TREE stopping rule: 100). Graphical editing was performed with FigTree version 1.4.2 (http://tree.bio.ed.ac.uk/software/figtree/). The genomic context of the genes coding for the protein sequences selected for the tree was explored based on the annotation of neighboring genes in the NCBI nucleotide repository. The number and position of conserved histidine residues relative to EMO of *S. aciditrophicus* was determined by manual inspection of the aligned amino acid sequences (see above).

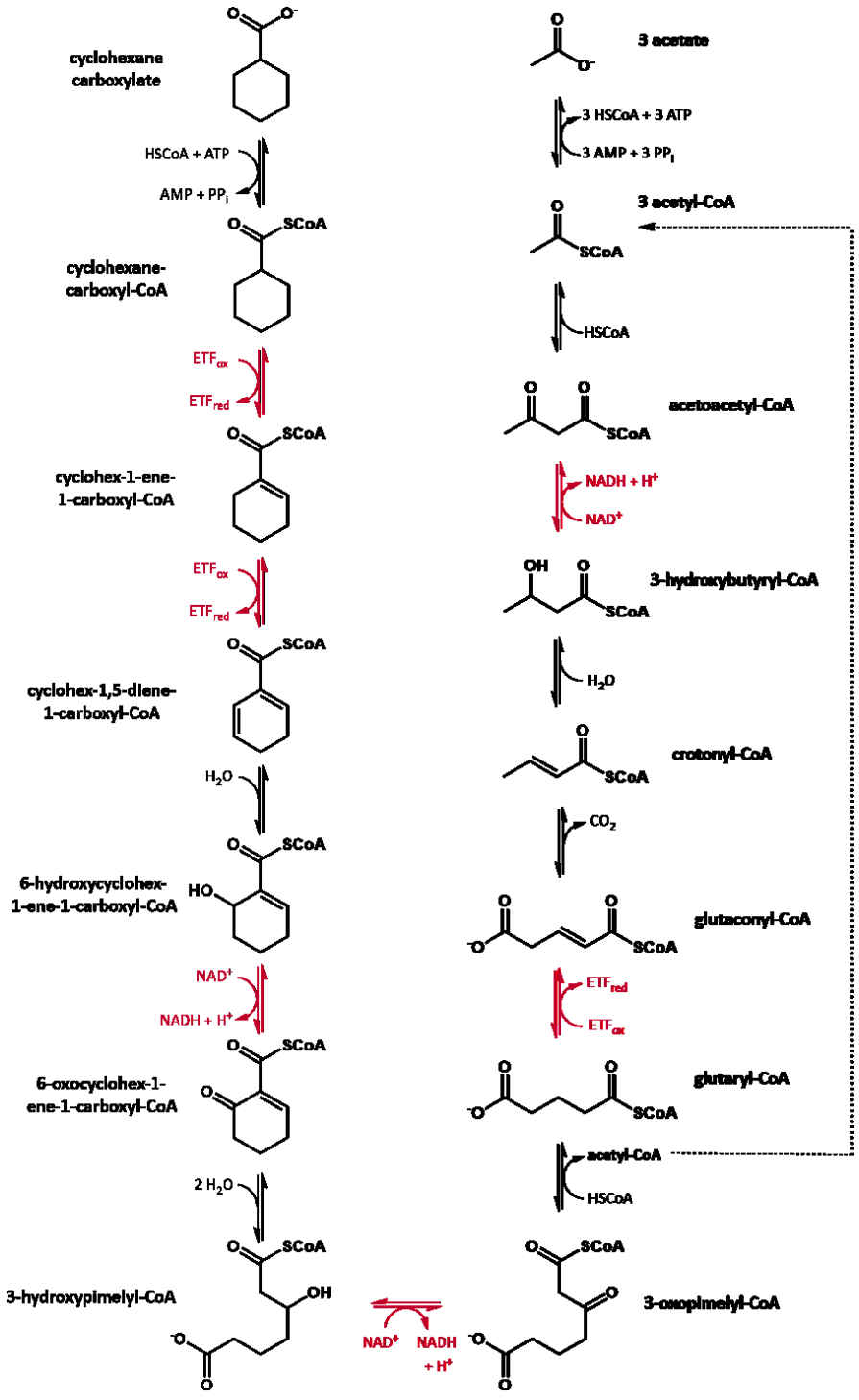

Fig. S1. Degradation of cyclohexane carboxylate to three acetate and one CO_2 by *S. aciditrophicus*. The β-oxidation sequence is initiated by cyclohexanoyl-CoA dehydrogenase (CHCoA DH). During syntrophic growth with CHC, the reducing equivalents formed (ETF_{red}, NADH) are re-oxidized by reduction of CO_2.

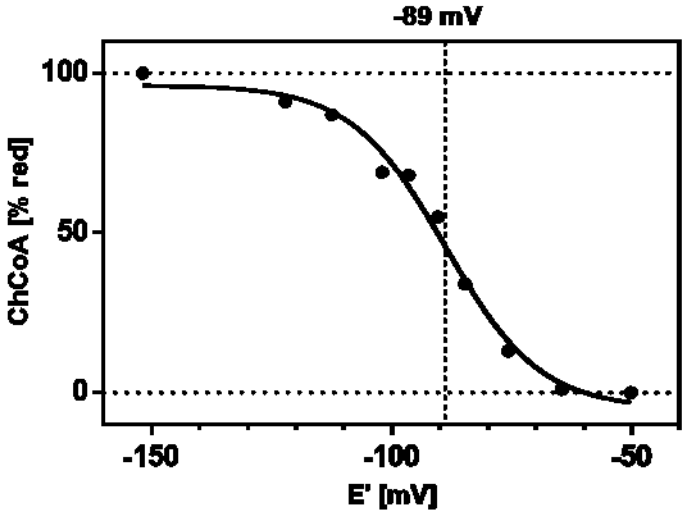

Fig. S2. Determination of the midpoint redox potential of the CHeneCoA/CHCoA redox pair. The concentration ratio of the CoA esters was determined via UPLC, the redox potential was determined from the absorption of added redox dyes of known redox potential. A fit to a Nernst curve is shown and the resulting midpoint potential is marked with a dashed line.

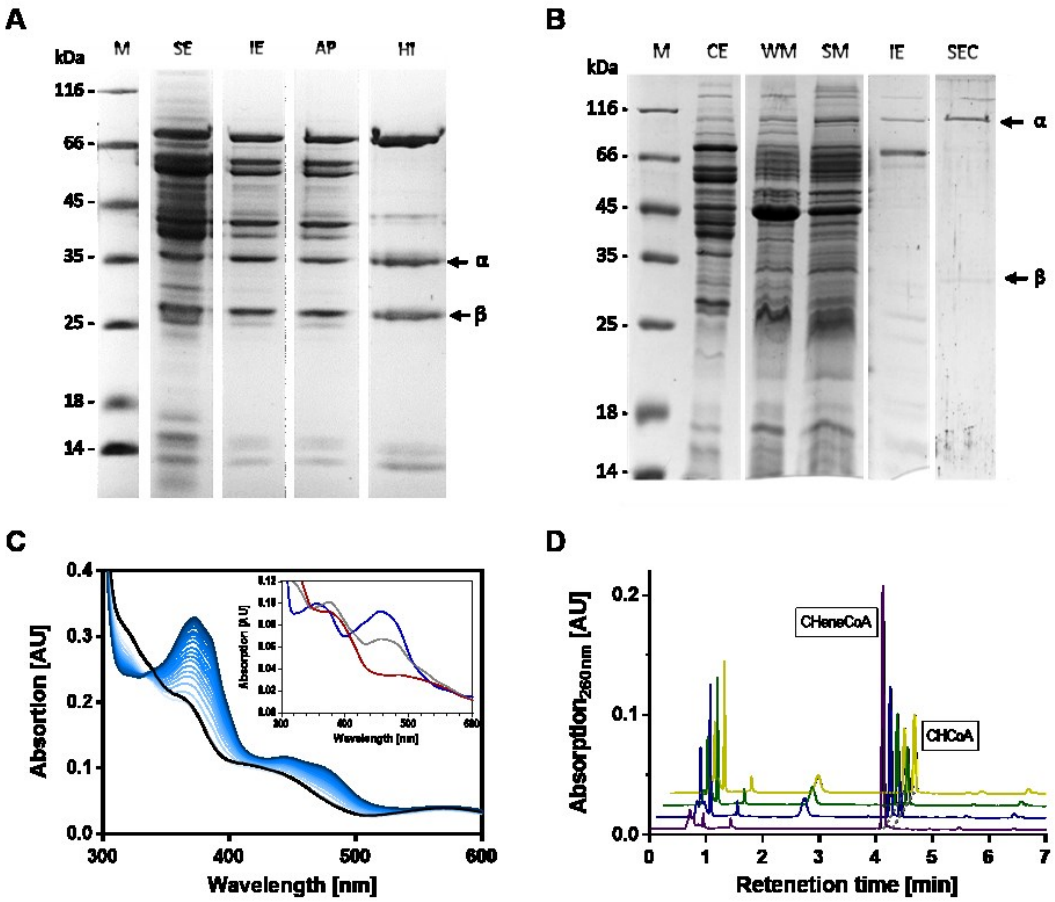

Fig. S3. Enrichment *(A)*, electron transfer reactions of ETF (*C, D*) and enrichment of mFDH (*B*) from *S. aciditrophicus. (A)* Enrichment of ETF from cells grown with crotonate. The respective α, and β-subunit (arrows) were identified by mass spectrometry. The abundant band migrating around 70 kDa was identified as subunit of acetyl-CoA synthetase (SYN_02635) that has no redox cofactor and did not interfere with electron transfer assays. *(B)* Enrichment of mFDH. The respective α, and β-subunit (arrows) were identified by mass spectrometry. The small γ-subunit escaped detection. M, mass standard; SE, soluble cell extract; IE, elution from anion-exchange chromatography; AP, supernatant after ammonium sulfate precipitation; HI, flow through of hydrophobic interaction chromatography; CE, crude cell extract; WM, washed membranes; SM, solubilized membranes; SEC, pooled fractions from size exclusion chromatography. *(C)* UV/vis spectra of ETF. Black line: ETF as isolated mainly in the reduced state; blue lines, spectra recorded in the presence of CHeneCoA/CHCoA DH every 60 s showing the stepwise oxidation to the red semiquinone ($FAD^{\bullet-}$, shoulder around 370 nm). Insert: blue line, fully oxidized; grey line, half-reduced semiquinone; red line, completely reduced hydroquinone. *(D)* UPLC analyses from samples taken during the ETF-, CHCoA DH-, and washed membrane fraction-dependent reduction of CHeneCoA to CHCoA by formate.

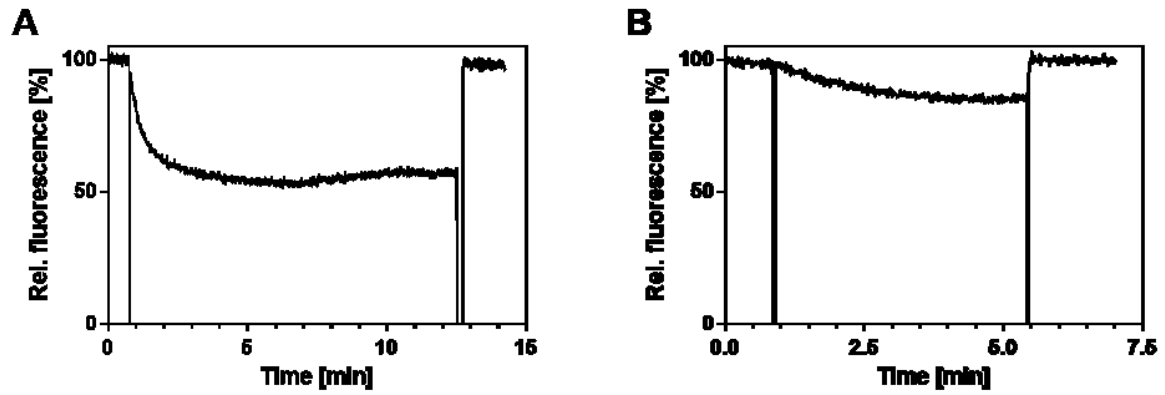

Fig. S4. ΔpH formation at inside-out membrane vesicles from *S. aciditrophicus*. The fluorescence quenching of 9-amino-6-chloro-2-methoxy acridine (ACMA) was followed after the addition of *(A)* ATP after 0.8 min, or *(B)* pyrophosphate after 0.8 min. Fluorescence quenching was abolished after addition of the protonophore nigericin after *(A)* 12.5 and *(B)* 5.4 min.

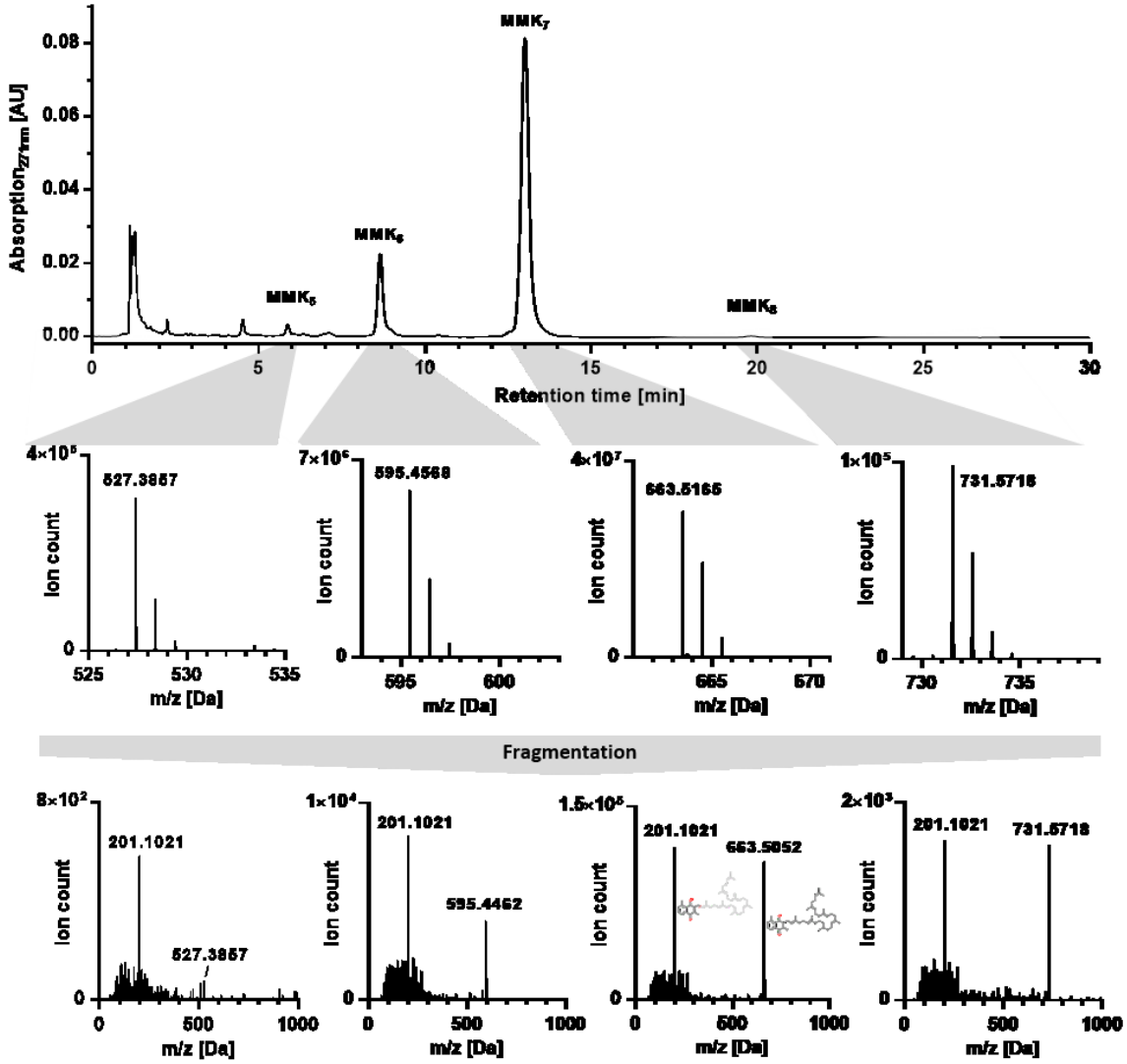

Fig. S5. Analyses of quinones from *S. aciditrophicus* membranes. Upper panel: UPLC elution profile of quinones with various isoprenoid chain lengths. Middle panel: ion chromatograms of individual quinone peaks as detected by ESI-QTOF-MS. Lower panel: fragmentation pattern showing the 2,3,6-trimethylnaphthoquinone peak after cleavage of the isoprenoid side chain.

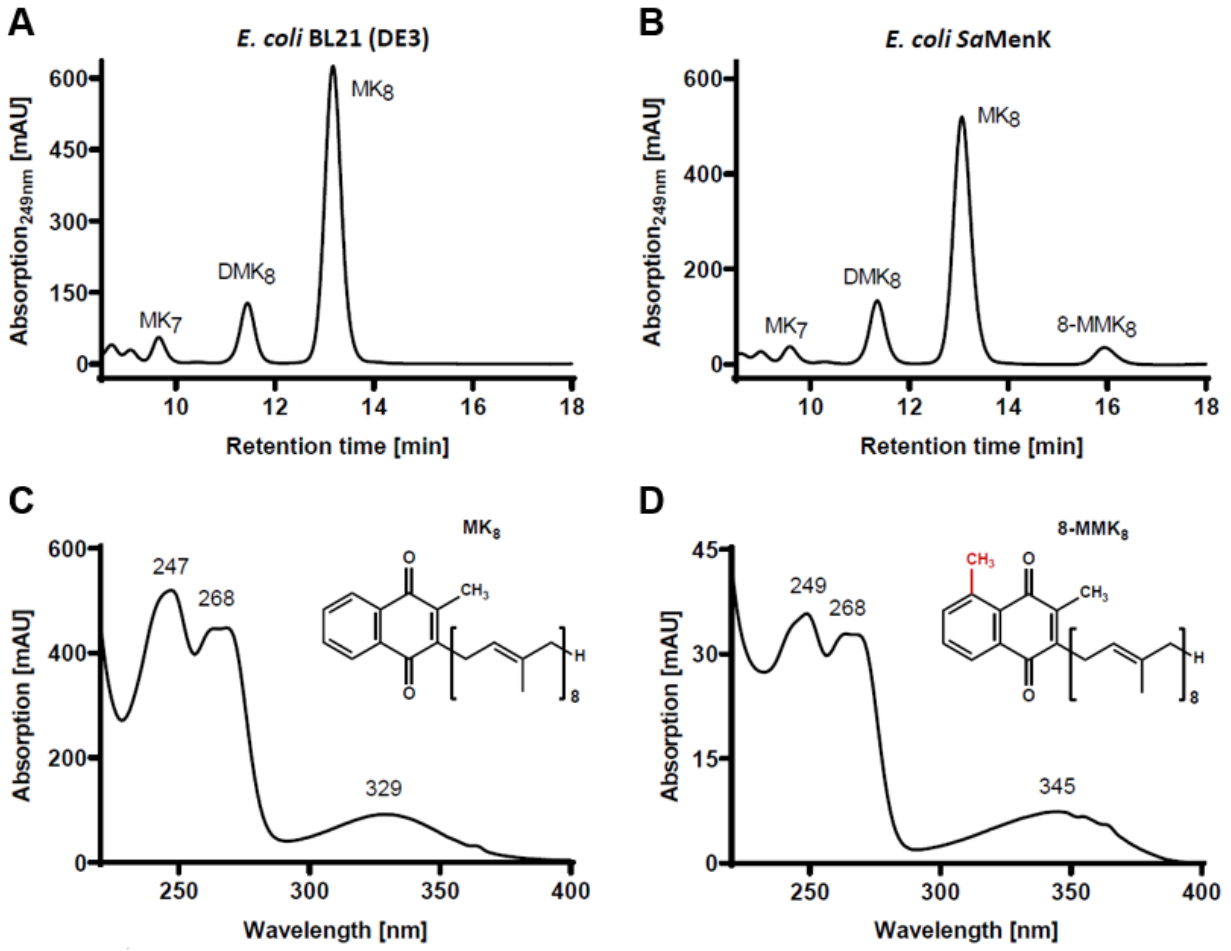

Fig. S6. Quinone profiles of *E. coli* BL21 (DE3) cells after production of the SYN_ 01802 gene product. Upper panel, HPLC elution profiles of extracted MK pool; lower panel UV/Vis spectra of MK_8 and 8-MMK_8 as indicated**.** *(A), (C) E. coli* BL21 (DE3) control wild type; *(B), (D) E. coli* BL21 (DE3) producing the SYN_01802 gene product.

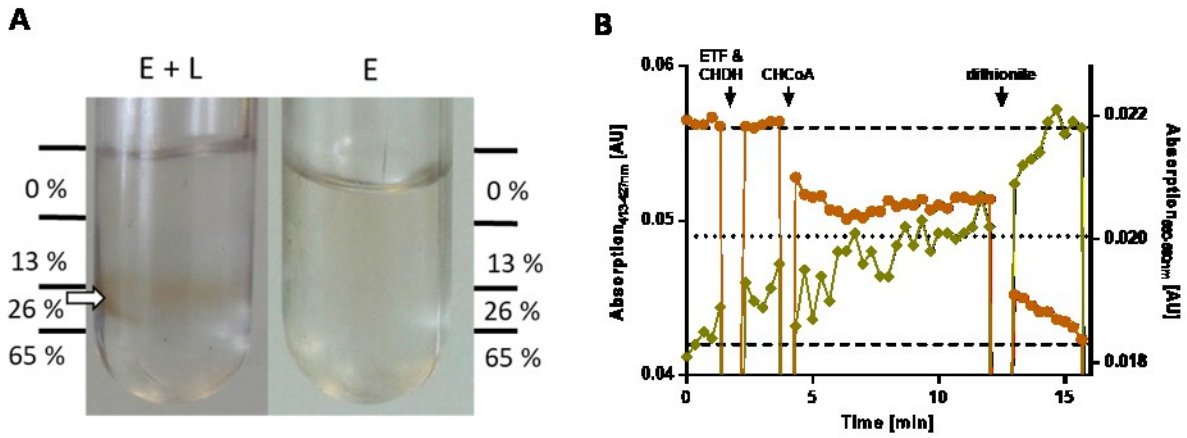

Fig. S7. Preparation and electron transfer reactions of EMO-containing proteoliposomes. *(A)* Sucrose gradient step gradient with EMO-containing proteoliposomes (E+L) and detergent-solubilized EMO (E). *(B)* Reduction of EMO, reconstituted in proteoliposomes, by CHCoA in the presence of ETF and CHCoA DH. Excess CHCoA reduced approximately one heme *b* equivalent. Light-brown circles represent data points of difference absorption 413 nm minus 427 nm, khaki diamonds of difference absorption 560 nm minus 580 nm.

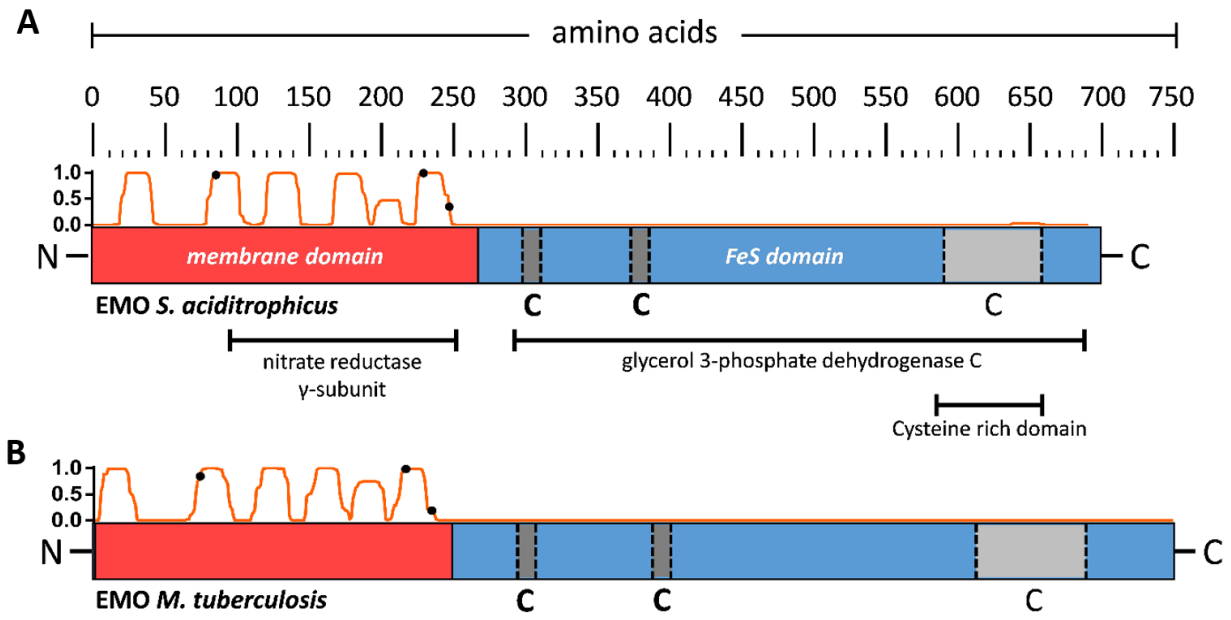

Fig. S8. Domain structure of EMO from *S. aciditrophicus (A)* and comparison with the one deduced from the genome of *M. tuberculosis (B)*, (gene id Rv0338c). *(A)* The N-terminal domain of EMO from *S. aciditrophicus* is predicted to contain five transmembrane helices (as shown by the TMHMM membrane score) and three His residues (marked by black circles) that are conserved among EMOs and other members of the nitrate reductase γ-subunit family. A sixth hydrophobic helix is not membrane-spanning. The C-terminal domain belongs to the glycerol-3-phosphate dehydrogenase (GlpC) family with two Fd-like and a cysteine-rich (sub)domain that are predicted to bind three [4Fe-4S] clusters (as indicated by a C). *(B)* Domain structure of EMO from *M. tuberculosis*. Amino acid sequence identities are 37%, the expect value during BLAST analysis is $2e^{-151}$.

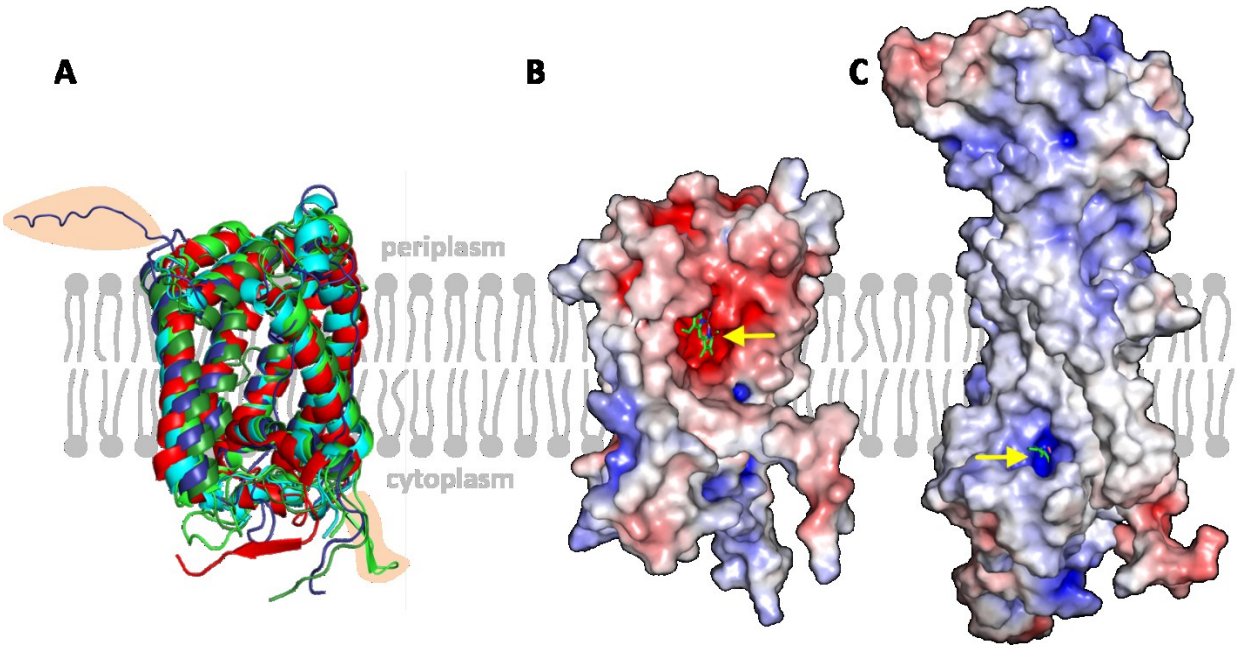

Fig. S9. Homology structure models of EMO and mFDH. *(A)* Structural alignment of all homology structure models of EMO (dark green, iTASSER; light green, SwissModel; light blue, Phyre2; dark blue, RaptorX) against the template NarI of *E. coli* (red, PDB: 1Q16). Light orange shaded parts lack a counterpart in the NarI sequence, as NarI is 45 amino acids shorter than the membrane domain of EMO. *(B)* Surface charge representation for EMO (SwissModel), and for *(C)* mFDH (iTASSER) from red (negative) to blue (positive; APBS Electrostatics plugin in PyMOL). Arrows mark the putative quinone binding sites. The positions of the distal heme molecule (green) in EMO and the HQNO molecule (cyan) in mFDH are adopted from the templates (PDB: 1Q16 and 1KQG, respectively).

References

1. N. Jacobsen, K. Torssell, Radikalische Alkylierung von Chinonen: Erzeugung von Radikalen in Redoxreaktionen. *Justus Liebigs Ann. Chem.* **763**, 135–147 (1972).
2. R. Schmid, F. Goebel, A. Warnecke, A. Labahn, Synthesis and redox potentials of methylated vitamin K derivatives. *J. Chem. Soc.* **8**, 1199–1202 (1999).
3. M. Willistein, *et al.*, Enantioselective Enzymatic Naphthoyl Ring Reduction. *Chem. - A Eur. J.* **24**, 12505–12508 (2018).
4. J. W. Kung, J. Seifert, M. von Bergen, M. Boll, Cyclohexanecarboxyl-coenzyme A (CoA) and cyclohex-1-ene-1-carboxyl-CoA dehydrogenases, two enzymes involved in the fermentation of benzoate and crotonate in Syntrophus aciditrophicus. *J Bacteriol.* **195**, 3193–3200 (2013).
5. U. K. Laemmli, Cleavage of structural proteins during the assembly of the head of bacteriophage T4. *Nature* **227**, 680–685 (1970).
6. M. M. Bradford, A rapid and sensitive method for the quantitation of microgram quantities of protein utilizing the principle of protein-dye binding. *Anal Biochem.* **72**, 248–254 (1976).
7. H. Schägger, G. von Jagow, Blue native electrophoresis for isolation of membrane protein complexes in enzymatically active form. *Anal. Biochem.* **199**, 223–231 (1991).
8. C. F. Goodhew, K. R. Brown, G. W. Pettigrew, Haem staining in gels, a useful tool in the study of bacterial c-type cytochromes. *BBA - Bioenerg.* **852**, 288–294 (1986).
9. D. Wilkens, R. Meusinger, S. Hein, J. Simon, Sequence analysis and specificity of distinct types of menaquinone methyltransferases indicate the widespread potential of methylmenaquinone production in bacteria and archaea. *Environ. Microbiol.*, 1462-2920.15344 (2020).
10. W. Lovenberg, B. B. Buchanan, J. C. Rabinowitz, Studies on the Chemical Nature of Clostridial Ferredoxin. *J. Biol. Chem.* **238**, 3899–3913 (1963).
11. E. A. Berry, B. L. Trumpower, Simultaneous determination of hemes a, b, and c from pyridine hemochrome spectra. *Anal. Biochem.* **161**, 1–15 (1987).
12. B. Poolman, *et al.*, "Amplified gene expression in Gram-positive bacteria, and membrane reconstitution of purified membrane transport proteins" in *Biological Membranes: A Practical Approach*, (2000).
13. S. F. Altschul, W. Gish, W. Miller, E. W. Myers, D. J. Lipman, Basic local alignment search tool. *J. Mol. Biol.* **215**, 403–410 (1990).
14. S. Lu, *et al.*, CDD/SPARCLE: the conserved domain database in 2020. *Nucleic Acids Res.* **48**, D265–D268 (2020).

15. E. L. L. Sonnhammer, G. von Heijne, A. Krogh, A hidden Markov model for predicting transmembrane helices in protein sequence. *Sixth Int. Conf. Intell. Syst. Mol. Biol.*, 8 (1998).
16. L. A. Kelley, S. Mezulis, C. M. Yates, M. N. Wass, M. J. E. Sternberg, The Phyre2 web portal for protein modeling, prediction and analysis. *Nat. Protoc.* **10**, 845–858 (2015).
17. A. Roy, A. Kucukural, Y. Zhang, I-TASSER: a unified platform for automated protein structure and function prediction. *Nat. Protoc.* **5**, 725–738 (2010).
18. A. Waterhouse, *et al.*, SWISS-MODEL: Homology modelling of protein structures and complexes. *Nucleic Acids Res.* **46**, W296–W303 (2018).
19. M. Källberg, *et al.*, Template-based protein structure modeling using the RaptorX web server. *Nat. Protoc.* **7**, 1511–1522 (2012).
20. Y. Huang, B. Niu, Y. Gao, L. Fu, W. Li, CD-HIT Suite: a web server for clustering and comparing biological sequences. *Bioinformatics* **26**, 680–682 (2010).
21. S. Kumar, G. Stecher, M. Li, C. Knyaz, K. Tamura, MEGA X: Molecular Evolutionary Genetics Analysis across Computing Platforms. *Mol. Biol. Evol.* **35**, 1547–1549 (2018).
22. J. Trifinopoulos, L.-T. Nguyen, A. von Haeseler, B. Q. Minh, W-IQ-TREE: a fast online phylogenetic tool for maximum likelihood analysis. *Nucleic Acids Res.* **44**, W232–W235 (2016).